Analysis of Implementation Methodologies of Deadbeat Direct-Torque and Flux Control (DB-DTFC) for IPMSMs in Stationary and Rotatory Reference Frames

Daniel E. Gaona
Applied Power Electronics Laboratory
University of Cambridge
Cambridge, UK
deg32@cam.ac.uk

Hadi El Khatib
Chair of Electrical Drives and Actuators (EAA)
Bundeswehr University Munich
Munich, Germany
hadi.khatib@unibw.de

Teng Long
Applied Power Electronics Laboratory
University of Cambridge
Cambridge, UK
tl322@cam.ac.uk

Michael Saur
Power Electronics Control
Audi AG
Ingolstadt, Germany
michael.saur@audi.de

***Abstract*— Deadbeat-control is a well-established control technique that uses the inverse machine model to determine the voltage commands required to achieve the desired torque and flux commands. Its classic implementation requires solving a quadratic equation with an extensive number of terms. Moreover, it can be only solved in the *dq*-reference frame. In this paper, two novel implementations are presented. The first methodology, in the dq-reference frame, reduces the algorithm's complexity and computation time. Moreover, it is immune to estimation errors of the permanent magnet flux. A second methodology based on the flux vector orientation is also presented. As opposed to the classic implementation, the proposed method does not require solving a quadratic equation; this reduces its complexity and computation time. Furthermore, the proposed methodology can be solved both in the dq and αβ frames since it relies only on the stator flux's magnitude and angle. Up to date and to the best of the author's knowledge, DB-DTFC in the stationary frame has not been presented before for salient machines. DB-DTFC in the stationary frame reduces the reliance on the position observer and facilitates the implementation of overmodulation techniques and six-step operation. The proposed methodology can operate in the MTPF line without any adjustments and it shows an adequate dynamic performance. Simulation and experimental results validate the methodologies. Caveats regarding their implementation are also discussed.**

Keywords—DB-DTFC, deadbeat, direct torque and flux control, IPMSM, permanent magnet, stationary, rotatory, implementation, control.

I. INTRODUCTION

Current-vector-control (CVC), Direct-torque-control (DTC), and model predictive control (MPC) are the most of common control strategies for interior-permanent magnet synchronous machines (IPMSM) used in traction applications [1]. CVC is the most popular of them due to its long-standing tradition. Although its performance is satisfactory for most applications, it is compromised near the DC-link and current limits. In contrast, DTC offers faster dynamics and higher DC-link utilization factors. However, it intrinsically results in variable switching frequency and undesirable torque ripple due to the hysteresis controller. Model predictive control (MPC) strategies usually require more computational throughput as compared to other techniques. However, as microcontrollers become more powerful and economical, MPCs' popularity has been increasing in the last decades. Among the MPC techniques, deadbeat direct torque and flux control (DB-DTFC) stands out as the most promising one [2]. This well-established control technique uses the inverse machine model to solve for the voltage inputs that would achieve the desired outcomes (in terms of torque and flux) in one switching period: "dead in one beat". DB-DTFC has been implemented in induction machines (IM) [2] [3], synchronous reluctance machines (SynRM) [4] [5], as well as in IPMSM [1] [6] [7] [8]. DB-DTFC offers many advantages. First, high dynamic performance can be achieved due to its intrinsic deadbeat nature. Second, it is more robust to parameter estimation errors as compared to CVC. Additionally, it can operate in the voltage and current limits without having to modify the control law. Finally, it can also lead to a reduction of the harmonic content and torque ripple [4].

The implementation of DB-DTFC for interior permanent magnet machines (IPMSMs) was first introduced in [1] and later in [8] and [9]. This classic implementation of DB-DTFC for IPMSMs is discussed in Section II. This method, however, requires solving a quadratic equation which consists of many terms. This complicates its implementation in real applications as the computational burden is not negligible. A *simplified* DB-DTFC methodology is derived and discussed in Section III. As opposed to the classic method, this deadbeat control law determines stator flux commands as opposed to voltage-commands. Thus, this methodology reduces the computational time and microcontroller processing power and simplifies the control structure. Moreover, this method is immune to permanent magnet estimation errors.

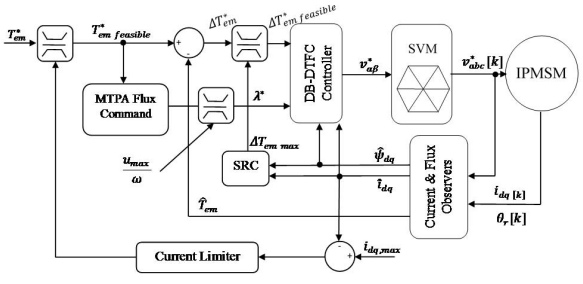

Figure 1: Complete DB-DTFC control scheme as in *[9]*. SRC: Square-root conditioning. MTPA: Maximum torque per ampere. SVM: Space-vector modulation.

Understanding DB-DTFC in terms of flux commands rather than voltage commands expands the design space for the controller. Section IV presents an alternative implementation of DB-DTFC whose control law is derived from the torque equation as a function of the stator flux's magnitude and angle. As opposed to the classic implementation, solving a quadratic equation is not required. Moreover, the proposed methodology can be applied both in the dq and $\alpha\beta$ frames. Up to date and to the best of the author's knowledge, implementation of DB-DTFC in the αβ-plane has not been presented for salient machines. Operation in the stationary reference frame reduces the reliance on the position observer and facilitates the implementation of strategies for overmodulation techniques and six-step operation. Experimental results in terms of command tracking and robustness to parameter estimation errors are shown in Section V. Experimental results are presented in Section VI.

II. DB-DTFC FOR IPMSM

DB-DTFC for IPMSMs, first introduced in [1], it is shown in Fig.1. Here, the torque and stator flux magnitudes are the control variables as it is commonly done in direct-torque-control (DTC) and MPC controllers. Due to the discrete nature of its implementation, a stator current observer and a stator flux observer are required to estimate the states of the machine. With this information, the algorithm solves the inverse torque equation to determine the voltage commands that satisfy both the flux magnitude $|\psi_s|^*$ and torque T_{em}^* requirements. The observers and the control law are described briefly in the next subsections. More details can be found in [1].

A. Current and Flux Observers

In general, the stator current is measured at the beginning of the PWM period, $[k-1]$, while the output voltage is only applied at the next switching cycle $[k]$. For consistency and to avoid instability problems, the calculation of the voltage command requires information about the state of the stator currents and flux in the time instant $[k]$. To cope with this time delay, dedicated observers are used.

For the stator current, a Luenberger-style current observer (LSCO) is generally used for DB-DTFC [1] [10]. The observer is implemented in the dq-reference frame as this frame facilitates the expression of the inherent saliency of IPMSMs. Several improvements to this observer have been implemented over the last two decades to enhance its accuracy. The state-of-the-art observer is shown in Fig.2. Here, $\tau = L_{dq}/R$ corresponds to the estimated stator time constants; ψ_{pm}, the permanent magnet flux; L_{dq}, the machine inductances; R, the stator resistance; whereas v and i are the

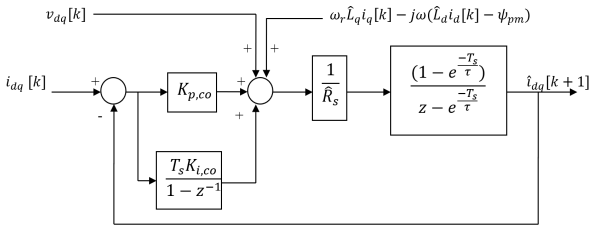

Figure 2: Representation of the Luenberger-style current observer in discrete-time and dq-reference frame.

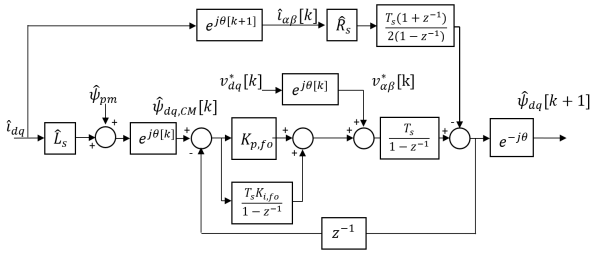

Figure 3: Representation of the Gopinath-style-flux-observer in dq and $\alpha\beta$ coordinates.

stator voltage and current, respectively. The factors $K_{i,co}$ and $K_{p,co}$ correspond to the integral and proportional PI-controller gains. The method for tuning these values is presented in [1]. They are selected according to the required bandwidth. The bandwidth ought to be high enough to track the current dynamics and, at the same time, low enough to avoid noise-induced tracking errors.

For the flux observer, a Gopinath-style flux observer (GSFO) is used. This observer combines the machine's current and voltage models. The voltage model is accurate at highs speeds but its more prone to errors at low speeds. The current model is sensitive to parameter estimation errors but, in general, more accurate than the voltage model at low speeds. The GSFO fuses these two models employing a PI controller ($K_{p,fo}$ and $K_{i,fo}$) which defines the transition between them as shown in Fig.3. The controller tuning is discussed in [10]. As a rule-of-thumb, during pole-placement, one of the poles is fixed at the desired transition frequency while the other is usually 10% of the first one [4].

B. Control Law Derivation

The IPMSM state equations in the dq-reference frame are shown in (1), (2), and (3) in vector form; i.e., $h_{dq} = h_d + j \cdot h_q$. The torque and differential-torque equations are shown in (4) and (5), respectively:

$$\rho\psi_{dq} = v_{dq} - Ri_{dq} - j\omega\psi_{dq} \tag{1}$$

$$\psi_d = L_d i_d + \psi_{pm}; \qquad \psi_q = L_q i_q \tag{2}$$

$$\rho i_d = \frac{p\psi_d}{L_d}; \qquad \rho i_q = \frac{p\psi_q}{L_q} \tag{3}$$

$$T_{em} = \frac{3P}{4}\left(\psi_d \cdot i_q - \psi_q \cdot i_d\right) \tag{4}$$

Here, ρ is the differential operator and P is the pole number. When the switching frequency f_s is larger than the fundamental frequency f_e, the differential terms can be discretized with the Euler's discretization method shown below:

$$\rho h_{dq} = \frac{\Delta h_{dq}}{Ts} = \frac{h_{dq}[k+1] - h_{dq}[k]}{T_s}$$

where T_s is the sampling period, $T_s = 1/f_s$. Applying Euler's discretization method, substituting (1) and (3) in (5), and rearranging the terms, a linear relationship between the stator voltages u_d and u_q at the instant [k] can be obtained as seen in (6). It is worth noting that all the terms in M and B correspond to the time instant [k] and are known (observed or measured) quantities. Eq. (6) corresponds to the line depicted in red in Fig.4a.

Classic DB-DTFC Implementation	Simplified DB-DTFC Implementation
$\rho T_{em} = \frac{3P}{4}\left(\rho\psi_d \cdot i_q + \psi_d \cdot \rho i_q - \rho\psi_q \cdot i_d - \psi_q \cdot \rho i_d\right)$ (5)	$\rho T_{em} = \frac{3P}{4}\left(\rho\psi_d \cdot \left(i_q - \frac{\psi_q}{L_d}\right) - \rho\psi_q \cdot \left(i_d - \frac{\psi_d}{L_q}\right)\right)$ (9)
$u_q[k] \cdot T_s = M \cdot u_d[k] \cdot T_s + B$ (6) $M = \frac{\psi_q[k](L_q - L_d)}{\psi_d[k](L_d - L_q) + \psi_{pm}L_q}$ $B = \left(\frac{L_qL_d}{(L_d - L_q)\psi_d[k] + L_q\psi_{pm}}\right)\left[\frac{4\Delta T_{em}^*}{3P} - \frac{\omega T_s}{L_dL_q}\left((L_q - L_d)(\psi_d^2[k] - \psi_q^2[k]) - L_q\psi_d[k]\psi_{pm}\right) - \frac{RT_s\psi_q[k]}{L_d^2L_q^2}\left((L_q^2 - L_d^2)\psi_d[k] - L_q^2\psi_{pm}\right)\right]$	$\psi_q[k+1] = M' \cdot \psi_d[k+1] + B'$ (10) $M' = \frac{L_q(L_d\, i_q[k] - \psi_q\,[k])}{L_d(L_q\, i_d[k] - \psi_d\,[k])}$ $B' = \psi_q[k] - \psi_d[k] \cdot M' - \frac{4\Delta T_{em}L_q}{3P(L_qi_d[k] - \psi_d[k])}$.
$\lvert\psi[k+1]\rvert^{*2} = \left(u_d[k]T_s - R_si_d[k]T_s + \omega T_s\psi_q[\mathrm{k}] + \psi_d[\mathrm{k}]\right)^2 + \left(u_q[k]T_s - R_si_q[k]T_s - \omega T_s\psi_d[\mathrm{k}] + \psi_q[k]\right)^2$ (7)	$\lvert\psi[k+1]\rvert^{*2} = (\psi_d[k+1])^2 + (\psi_q[k+1])^2$ (11)
$B_{\max} = \lvert\psi_s[k+1]\rvert^* \cdot \sqrt{1+M^2} + M \cdot x - y$ $B_{\min} = -\lvert\psi_s[k+1]\rvert^* \cdot \sqrt{1+M^2} + M \cdot x - y$ (8)	$B'_{\max} = -B'_{\min} = \psi^* \cdot \sqrt{M'^2 + 1}$ (12)

Any combination of $(u_d[k], u_q[k])$ along this line will produce the desired differential torque ΔT_{em}^* in one switching cycle. To select the appropriate combination, a second constraint is required. The stator flux magnitude $|\psi[k+1]|^*$ in (7) is used for this purpose. While (6) depicts a line, (7) depicts a circle (Fig.4a) and the points of intersection between them define the stator voltage commands. Solving a quadratic equation ($ax^2 + bx + c = 0$) is required to find the aforementioned intersections.

C. Maximum Torque per Flux

The control law in Section II.B assumes that the flux and torque commands can be both simultaneously satisfied. However, when the torque command is higher than the maximum torque achievable with a certain flux (MTPF), DB-DTFC fails to find a solution as the line and circle equations do not intersect at any point. This is particularly the case during flux-weakening II. To avoid this, ΔT_{em} can be limited as in [3] to ensure a feasible torque command and/or prevent over-currents. Alternatively, an overlap between the circle and the line equations can be enforced by making the torque line (6) tangent to the flux circle (7) [9]. This can be achieved by ensuring that the line-intercept B in (6) remains within B_{min} and B_{max} in (8). This strategy is referred to as as *square-root conditioning* (SRC) as (8) is obtained by equating the discriminant of the DB-DTFC's quadratic equation to zero [9].

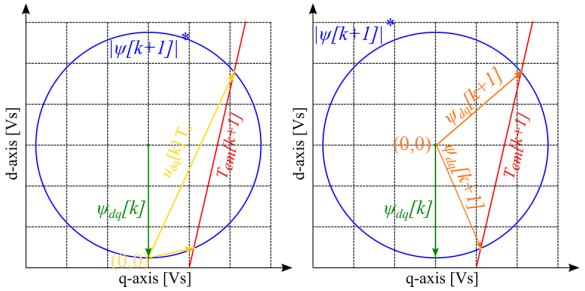

a) Voltage-Sec Plane b) Flux Plane

Figure 4: Graphical Representation of the a) standard and b) simplified DB-DTFC methods.

III. Simplified DB-DTFC Implementation

Eq. (6) and (7) are each formed of many terms which complicates the calculation of their intersection. To simplify the computation efforts, some authors disregard the voltage drop in the stator resistor. This, however, compromises the accuracy of the control algorithm. A simpler methodology is introduced in this section.

A. Control Law Derivation

Substituting (3) in (5), the differential torque equation can be defined as a function of $\rho\psi_{dq}$ as shown in (9). Applying Euler discretization method and rearranging the terms, a linear relationship between ψ_d and ψ_q at the time instant [k+1] can be obtained, as seen in (10). When comparing (6) to (10), the reduction in complexity is clear. Moreover, the flux command, previously described in (7) as a circle not centered at the origin, is no longer required. Contrarily, (11) can be directly used. While (10) depicts a line, (11) depicts a circle centered at zero and the point of intersection between these two lines defines the desired ψ_d and ψ_q in the time instant [k+1] as shown in Fig.4b. Thereafter, the voltage commands are then computed as in (13):

$$u_d^*[k] = \left(\frac{\psi_d[k+1] - \psi_d[k]}{T_s}\right) + Ri_d[k] - \omega\psi_q[k] \quad (13.1)$$

$$u_q^*[k] = \left(\frac{\psi_q[k+1] - \psi_q[k]}{T_s}\right) + Ri_q[k] + \omega\psi_d[k] \quad (13.2)$$

By separating the computation of the voltage from the flux, the complexity and number of the calculations reduce drastically. The transient and steady-state behaviors are identical to the ones obtained with the standard DB-DTFC implementation as seen in the next section.

B. Maximum Torque per Flux (MTPF)

Similar to what is done in [9], making sure that B remains between $B_{\max}$ and $B_{\min}$ ensures a feasible solution of DB-DTFC and MTPF operation in steady-state. These limits are calculated in (12). As compared to (8), only one equation is needed since $|B'_{max}| = |B'_{min}|$. Moreover, (12) is more compact which reduces the computation burden of the algorithm even further.

IV. DB-DTFC FOR IPMSMS IN THE STATIONARY $\alpha\beta$-REFERENCE FRAME

The implementation of the DC-DTFC algorithm for IPMSMs in the stationary reference frame is difficult due to the saliency and the fact that the stator flux is not directly proportional to the stator current due to the permanent magnet flux ψ_{pm}. One could attempt to rotate the line equation (6) by θ [rad] (the angle between the $\alpha\beta$ and the dq reference frames). However, for specific values of θ, the rotation would yield a vertical line in the $\alpha\beta$-plane. The slope-intercept representation of a line fails to characterize vertical lines as, in such cases, both the slope and the intercept converge to infinity. A different methodology is therefore necessary. A different methodology to cope with this problem is presented in the next section.

V. DB-DTFC USING FLUX MAGNITUDE AND PHASE

In this section, a different implementation of the DB-DTFC is presented. Contrary to what is done in the classic DB-DTFC implementation presented in Section II, the torque equation is here defined as a function of the stator flux magnitude and phase, as seen in (25):

$$T = \frac{3P}{4}\left(\frac{\psi_{pm}\sin\delta}{L_d}|\psi| + \frac{L_d-L_q}{L_dL_q}\cdot\frac{\sin 2\delta}{2}\cdot|\psi|^2\right) \quad (25)$$

where $|\psi|$ corresponds to the stator flux magnitude and δ to the angle between $\psi_{\alpha\beta}$ and ψ_{pm} (aligned with the d^+-axis). Fig.5 depicts (25) for different values of $|\psi|$ and δ. It is worth noting that not all the curves are monotonically increasing. Contrarily, they reach local maximum and minimum points at different values of δ. For values of $|\psi|$ less than or equal to $\left[\psi_{pm}\cdot L_q/(L_q-L_d)\right]$, (25) has only two local maximum/minimum points. These points can be estimated through (26):

$$|\delta_{\max}| = \operatorname{acos}\left(\xi - \sqrt{\xi^2+0.5}\right) \quad (26)$$

where:

$$\xi = \frac{\psi_{pm}\cdot L_q}{4\cdot|\psi|^*\cdot(L_q-L_d)} \quad (27)$$

For values of $|\psi_s|$ larger than $\left[\psi_{pm}\cdot L_q/(L_q-L_d)\right]$, two extra inflection points appear whose local maximums are given by (28):

$$|\delta_{\min}| = \pm\operatorname{acos}\left(\xi + \sqrt{\xi^2+0.5}\right) \quad (28)$$

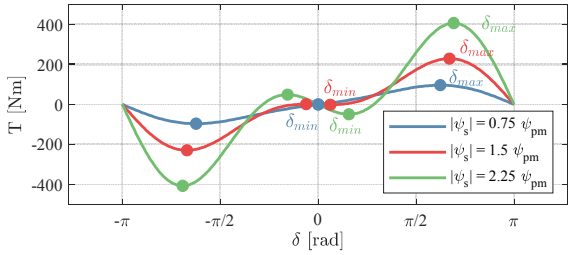

Figure 5: Torque as a function of the stator flux amplitude $|\psi_s|$ and angle δ. $(\cdot)$ depicts the local maximums and minimums.

Between $|\delta_{\min}|$ and $|\delta_{\max}|$, the torque is monotonically increasing ($\delta > 0$) or decreasing ($\delta < 0$). For values of $|\psi_s|$ less or equal to $\left[\psi_{pm}\cdot L_q/(L_q-L_d)\right]$, $|\delta_{\min}|$ is zero.

A. Control Law Derivation

The differential torque equation in (29) is derived from (25).

$$\rho T_{em} = \frac{3P}{4}\left[\left(\frac{\psi_{pm}|\psi|}{L_d}\cos\delta + \frac{L_d-L_q}{L_dL_q}\cos 2\delta\,|\psi|^2\right)\cdot\rho\delta + \left(\frac{\psi_{pm}}{L_d}\sin\delta + \frac{L_d-L_q}{L_dL_q}\sin 2\delta\,|\psi|\right)\cdot\rho|\psi|\right] \quad (29)$$

Here, the differential terms $\rho|\psi|$, ρT_{em}, and $\rho\delta$ can be discretized with Euler's method as shown in (30):

$$\frac{\Delta T_{em}}{T_s} = \frac{3P}{4}\left(\frac{\psi_{pm}|\psi_s|}{L_d}\cos\delta + \frac{L_d-L_q}{L_dL_q}\cos 2\delta\,|\psi_s|^2\right)\cdot\frac{\Delta\delta}{T_s} + \left(\frac{\psi_{pm}}{L_d}\sin\delta + \frac{L_d-L_q}{L_dL_q}\sin 2\delta\,|\psi_s|\right)\cdot\frac{\Delta|\psi_s|}{T_s} \quad (30)$$

In the classic DB-DTFC implementation, the flux command $|\psi[k+1]|^*$ defines the circle equation (7). Here, however, the flux command is directly satisfied by considering $\Delta|\psi_s| = |\psi[k+1]|^* - |\psi[k]|$. Consequently, $\Delta\delta$ can be directly calculated with (31).

$$\Delta\delta = -\frac{M''}{N''}\cdot\Delta|\psi| + \frac{4\Delta T_{em}}{3PN''} \quad (31)$$

where:

$$M'' = \frac{\psi_{pm}}{L_d}\sin\delta + \frac{L_d-L_q}{L_dL_q}\sin 2\delta\,|\psi| \quad (32)$$

$$N'' = \frac{\psi_{pm}|\psi|}{L_d}\cos\delta + \frac{L_d-L_q}{L_dL_q}\cos 2\delta\,|\psi|^2 \quad (33)$$

Eq. (31) is explicit and linear. As opposed to the classic DB-DTFC implementation, solving a quadratic expression is not required. This reduces the complexity of the implementation and its computation time. Moreover, the proposed methodology can be applied both in dq and $\alpha\beta$ frames since it relies only on the stator flux's magnitude and angle. The flux magnitude is independent of the reference frame; i.e., $|\psi_{dq}| = |\psi_{\alpha\beta}| = |\psi|$. Likewise, the flux angle can be straightforwardly converted from one reference frame to the other: $\delta = \gamma - \theta$; where γ is the flux angle in the $\alpha\beta$-plane.

After solving for $\Delta\delta$, the values of ψ_d and ψ_q at the time instant [k+1] are known and the voltage commands are then computed as in (34)-(35) in the dq-reference frame or as in (37)-(38) in the $\alpha\beta$-reference frame:

$$u_d^*[k] = \left(\frac{|\psi|^*\cos(\delta[k]+\Delta\delta)-\psi_d[k]}{T_s}\right) + Ri_d[k] - \omega\psi_q[k] \quad (34)$$

$$u_q^*[k] = \left(\frac{|\psi|^*\sin(\delta[k]+\Delta\delta)-\psi_q[k]}{T_s}\right) + Ri_q[k] + \omega\psi_d[k] \quad (35)$$

$$u_\alpha^*[k] = \left(\frac{|\psi|^*\cos(\gamma[k]+\Delta\delta+\omega T_s)-\psi_\alpha[k]}{T_s}\right) + Ri_\alpha[k] \quad (37)$$

$$u_\beta^*[k] = \left(\frac{|\psi|^*\sin(\gamma[k]+\Delta\delta+\omega T_s)-\psi_\beta[k]}{T_s}\right) + Ri_\beta[k] \quad (38)$$

The term ωT_s in (37) and (38) compensates for the rotation of the permanent magnet flux in one time instant. Alternatively, a position observer such as the Enhanced-Luenberger-Style position observer can be used. Hereon, only the implementation in the $\alpha\beta$-plane will be analyzed.

This control strategy share some similarities with the control strategies presented in [11] and [12]. These strategies do implement direct flux control; however, the torque is not controlled in closed-loop. Contrarily, the torque equation (25) is expressed as a function of the i_q current which is in turn actively controlled in closed-loop. This permits to limit the current more easily. In DB-DTFC, an outer control loop is required to limit the current. The current limiter is described in [9] and shown in Fig.1.

B. Practical Implementation Issues

To avoid a division by zero, it is recommended to setup minimum value for $|N''|$. Additionally, it is important to ensure that the commanded flux angle $\delta[k+1]$ remains between $|\delta_{\min}|$ and $|\delta_{\max}|$. In this range, the differential torque equation is strictly positive. For most applications, the flux command $|\psi|^*$ follows the *maximum torque per ampere* (MTPA) line. Since $|\psi|^*$ increases proportionally to the torque command T^*, the required δ is never close to $|\delta_{\min}|$. Thus, minor inaccuracies in the estimation of $|\delta_{\min}|$ caused by parameter estimation errors are relatively unimportant. Contrarily, in the flux-weakening region or for large torque commands, the required δ can be close to $|\delta_{\max}|$. The MTPF operation is discussed in the next section.

C. Maximum Torque per Flux (MTPF)

The tangent point between the circle and line equation in the classic implementation of DB-DTFC corresponds to $|\delta_{\max}|$ in Fig.5. Theoretically, MTPF can be achieved with this implementation without further adjustments. In practice, however, as δ approaches $|\delta_{\max}|$, the differential torque equation $\partial T_{em}/\partial\delta$ in (9) converges to zero and its inverse, $\partial\delta/\partial T_{em}$, to infinity. Given that the sensitivity of the controller is proportional to $\partial\delta/\partial T_{em}$, noise and other disturbances can cause large torque oscillations. In this paper, $\partial\delta/\partial T$ was limited via a hard-saturation limit when the estimated angle δ found itself in the vicinity of δ_{max}. This reduced the oscillations and allowed the system to operate in the entire torque-speed range without stability problems. As a drawback, the control bandwidth is reduced in this region. Alternative methodologies to ensure operation at the MTPF (MTPV) line can be found in [11] and [12]. The selection of the optimal strategy was out of the scope of this research.

D. Torque Deviation due to Parameter Estimation Errors at the MTPF Line

As it is common for all DB-DTFC implementations, the proposed method is based on the differential torque equation. That is, the algorithm will track the commanded torque even in the presence of parameter estimation errors. This is true for all operating regions except for the MTPF. Parameter estimation errors might affect the ability of the controller to track the exact MTPF torque. Fig.6 shows the effect of the errors in the estimation of the machine inductances and permanent magnet flux. Whereas overestimations of L_q have a minimum influence on the torque accuracy, its underestimation has a greater impact. Both under and overestimations of L_d, on the other hand, result in torque deviations but limited to less than 1%. Errors in the estimation of the permanent magnet flux result both in torque deviations. However, even for an 80% error, the torque deviation remains below 3%. The reason for such a small error is because $\partial T_{em}/\partial\delta$ is close to zero in the vicinity of δ_{max}. Thus, small deviations of δ have a minimum impact on the torque. Similar results are obtained for the standard DB-DTFC implementation as shown in [9].

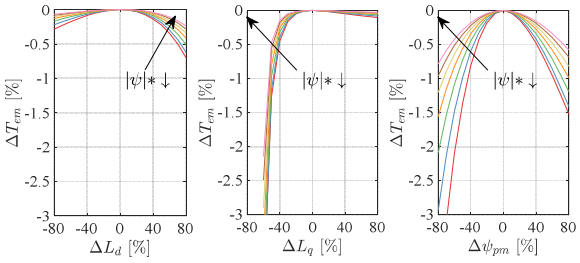

Figure 7: Torque as a function of the stator flux amplitude $|\psi_s|$ and angle δ. $(\cdot)$ depicts the local maximums and minimums.

I. Results

The standard, simplified, and the implementation based on the flux magnitude and angle $(\psi-\delta)$ of DB-DTFC are evaluated first via simulations and later experimentally. The experimental setup consists of 300kW IPMSM.

A. Deadbeat Response

Fig.7 shows the deadbeat response of the classic and simplified implementations. There is not an important difference between them. For all the methods, the deadbeat response will be achieved whenever is possible. For large torque commands, more than one sampling instant would be required. This is presented in the next section.

B. Transient Behavior

Simulation results of the step-response of the different DB-DTFC implementations are shown in Fig.8. The different implementations yield almost identical trajectories during the transient. During field weakening II, all the methods follow the MTPF line in steady-state, as seen in Fig.6b). The implementations based on the flux magnitude and angle show a faster response as they fixed the flux angle at $\delta_{\max}$ while the classic method converges more gradually to this value due to the SRC.

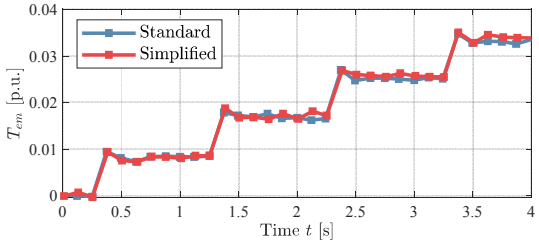

Figure 6: Deadbeat response achieved with the standard/classic DB-DTFC implementation and the simplified method.

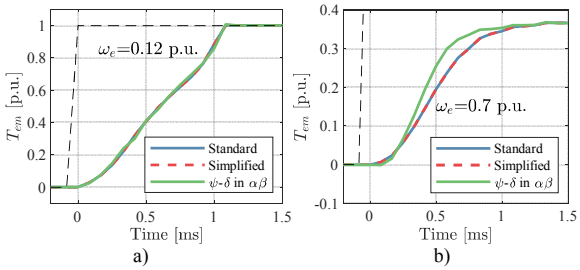

Figure 8: Step-response achieved with all the algorithms at different speeds: a) 0.12 p.u. and b) 0.7 p.u. These values are normalized to the maximum rotor speed and not to the rated speed.

Fig.9 shows experimental results to validate the simulation. Complex current-vector control (CVC) is also included for comparison. Its bandwidth is much lower than that of the deadbeat controllers. As predicted by the simulation, the rated torque is achieved in approximately 1ms. All the methods show a similar response even though the trajectories vary slightly from one to the other. Since all the methods use the same observers, the flux magnitude and angle in steady-state are the same regardless of the method.

C. *Torque-Speed Range*

Fig.10 shows torque-speed measurements of the machine with different DB-DTFC implementations. As seen in Fig.10a, there is not a considerable difference between them. All the methods follow the same trajectory. The slight reduction of the torque seen during the interval 10s-15s in Fig.10a, is due to the de-rating strategy. This is implemented as part of the safety control system of the testbench. Since all the algorithms were tested approximately at the same temperature, the derating has an equal influence on all the controllers.

Although the standard and simplified methods are almost identical (Fig.10b), the implementation of DB-DTFC based on $|\psi| - \delta$ is different at the beginning of the MTPV line. Although this difference can be partially attributed to derating, it is more likely due to the MTPF strategy discussed

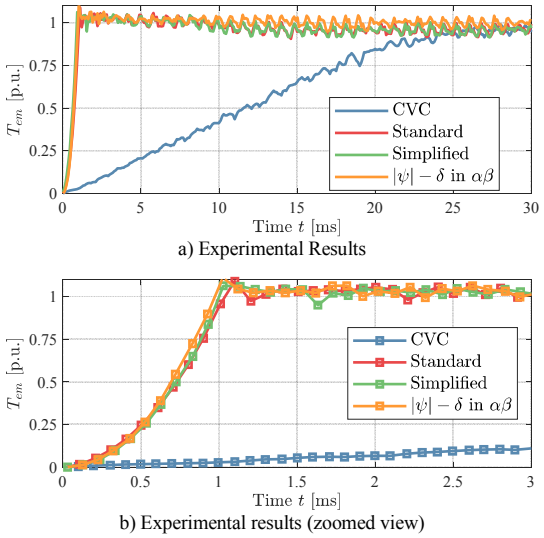

Figure 9: Measured step-responses for different control algorithms at the speed of $\omega_e = 0.25$ p.u. normalized with respect to the maximum speed.

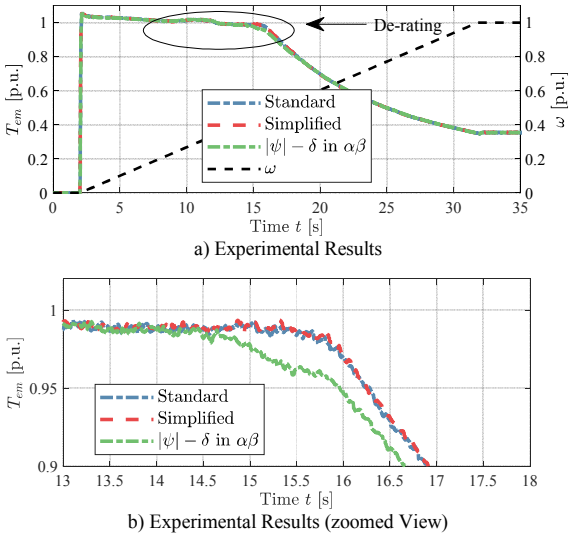

Figure 10: Torque and Speed characterization of the IPMSM using different DB-DTFC control strategies presented in this paper.

in Section V.C. Enhanced MTPF strategies such as the ones used in [11] and [12] could improve the performance. This needs to be studied more in detail in future works.

D. *Response to Parameter Estimation Errors*

1) *Stator Inductances and Resistance*

At low speeds, parameter estimation errors change the control effort of the controller. Increasing $\hat{L}_d$ or decreasing $\hat{L}_q$ reduces the rise-time but it can lead to oscillations in the steady-state that decay with time. Contrariwise, decreasing $\hat{L}_d$ or increasing $\hat{L}_q$ decelerates the transient performance. The stator resistance has a minimum impact on the system.

At higher speeds, in the FW region, parameter estimation errors result in torques that are lower than the MTPF torque. However, the torque deviations are small as discussed in Section V.D. Unless the error is considerably large, estimation errors in the inductance and resistance do not affect the stability of the state response nor the capability of the system to operate at zero torque. This is different for errors in the estimation of the permanent magnet flux as seen in the next section.

2) *Permanent Magnet Flux ψ_{pm}*

Fig.11 shows torque transient and steady-state response of the different DB-DTFC implementations when subjected to inaccurate estimations of the permanent magnet flux ψ_{pm}. The simplified implementation of DB-DTFC does not depend on the value of ψ_{pm}. Consequently, its operation is unaffected by ψ_{pm} estimation errors; the other two methods are however affected. An over-estimation of ψ_{pm}, Fig.11b), increases slightly the rise-time of the standard and $|\psi| - \delta$ methods. However, the system is still stable and can operate at low and zero torque commands. Underestimating the permanent magnet flux, on the other hand, shows a different effect. First, the rise time of all the methods is reduced as the controllers react more aggressively to torque and flux errors.

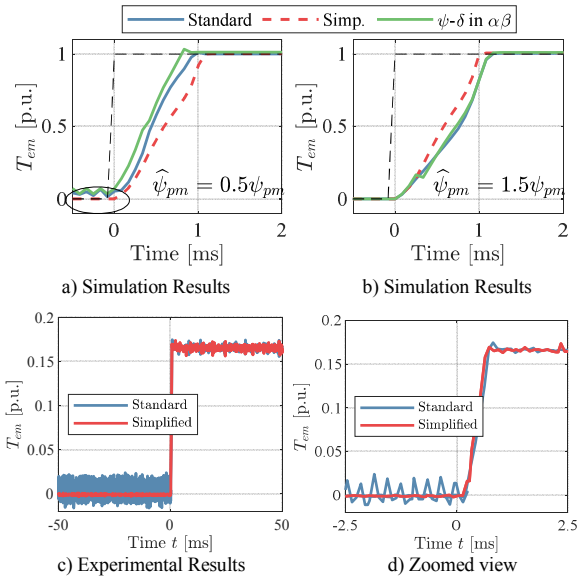

Figure 11: Torque step response under permanent magnet estimation errors for the different DB-DTFC implementations. $\omega_e = 0.25$ p.u. a) Simulation results, underestimation of ψ_{pm}. b) Simulation results, overestimation of ψ_{pm}. c)-d) Experimental results, underestimation of ψ_{pm}.

This, however, causes stability problems at low and zero torques as shown in Fig.11a. This issue was validated experimentally as shown in Fig.11c and Fig.11d.

Thus, over-estimation of ψ_{pm} is preferred over underestimations. In general, ψ_{pm} is inversely proportional to the temperature. Thus, during operation the value of ψ_{pm} will tend to decrease. This will lead to overestimations of ψ_{pm} which are less harmful. Both underestimation and overestimation of the PM flux will result in torques lower than the MTPF torque as discussed in Section V.C.

II. Discussions

1) Simplified DB-DTFC implementation

The simplified implementation reduces the computation time of the control algorithm. It shows an identical dynamic performance than the standard method in terms of command tracking. Moreover, it is more robust to parameter estimation errors as the ψ_{PM} is not needed for the computation of the voltage commands.

The simplified implementation still relies on the current and flux observers which in turn depend, to a certain degree, on the estimation of ψ_{PM}. The current model of the GSFO requires an estimation of ψ_{PM}. As a result, estimation errors of ψ_{PM} will affect the accuracy of the flux estimation but only at low speeds while the current-model is dominant. At high speeds, the voltage model dominates and the impact of ψ_{PM} on the flux accuracy is minimum. For the current observer (LSCO) shown in Fig.2, the ψ_{PM} is not directly used. However, LSCO uses the flux estimations from the GSFO. Thus, inaccuracies in the GSFO caused by estimation errors of ψ_{PM}, influence the LSCO as well. Nonetheless, this influence is seen only during transients as the LSCO is implemented in the *dq*-reference frame. Thus, the steady-state current estimation is unaffected,

Whereas the classic implementation depends both directly and indirectly on the estimation of the permanent magnet flux, the simplified implementation only depends indirectly through the observers. Thus, the simplified method is more robust particularly at high speeds where both the LSCO and GSFO are almost independent of ψ_{PM}.

2) DB-DTFC as a function of $|\psi| - \delta$

DB-DTFC as a function of $|\psi| - \delta$ is stable and operates during the entire torque-speed range. The deadbeat response and the command tracking capabilities are comparable to those of the standard DB-DTFC. Moreover, this implementation allows for a seamless integration with six-step strategies such as the deadbeat flux control (DBFC) discussed in [13], [14], and [15]. There are however some drawbacks that need to be considered. First, this implementation requires a considerable amount of trigonometric functions as seen in (30)-(33). The computation effort required is higher than for the standard or simplified implementations. Moreover, as seen in Fig.10b, the operation at the MTPF line presents a challenge since at this point, $\partial\delta/\partial T$ tends to infinity. Several methods can be used to address this problem at the expense of more complexity and computational effort.

III. Conclusions

In this contribution, different implementation methods of DB-DTFC for IPMSM were analyzed. The main conclusions are listed below:

- The implementation of the DB-DTFC algorithm can be simplified when considering the fluxes and not the voltages as variables. This simplified implementation reduces the computational time and complexity of the algorithm.
- The simplified method has almost identical command-tracking performance as the standard DB-DTFC implementation.
- The simplified implementation is more robust to errors in the estimation of the permanent magnet flux magnitude, particularly, at high speeds.
- DB-DTFC can be implemented in the αβ-plane if the torque as a function of the flux magnitude and angle ($\psi - \delta$) is considered. This allows for seamless integration with six-step control strategies.
- DB-DTFC as a function of |ψ|-δ shows a dynamic performance comparable to that of the standard DB-DTFC. However, it requires several trigonometric functions that demand a higher computational burden.
- The operation of DB-DTFC as a function of |ψ|-δ near the MTPF line must be carefully addressed as the control sensitivity increases considerably at this point.

IV. References

[1] J. S. Lee, C. Choi, J. Seok, and R. D. Lorenz, "Deadbeat-Direct Torque and Flux Control of Interior Permanent Magnet Synchronous Machines With Discrete Time Stator Current and Stator Flux Linkage Observer," in IEEE Transactions on Industry Applications, vol. 47, no. 4, pp. 1749-1758, July-Aug. 2011, doi: 10.1109/TIA.2011.2154293.

[2] R. D. Lorenz, "The emerging role of dead-beat, direct torque and flux control in the future of induction machine drives," 2008 11th International Conference on Optimization of Electrical and Electronic Equipment, Brasov, 2008, pp. XIX-XXVII, doi: 10.1109/OPTIM.2008.4602331.

[3] B. H. Kenny and R. D. Lorenz, "Stator- and rotor-flux-based deadbeat direct torque control of induction machines," in IEEE Transactions on Industry Applications, vol. 39, no. 4, pp. 1093-1101, July-Aug. 2003, doi: 10.1109/TIA.2003.813727.

[4] M. Saur, D. E. Gaona Erazo, J. Zdravkovic, B. Lehner, D. Gerling, and R. D. Lorenz, "Minimizing Torque Ripple of Highly Saturated Salient Pole Synchronous Machines by Applying DB-DTFC," in IEEE Transactions on Industry Applications, vol. 53, no. 4, pp. 3643-3651, July-Aug. 2017, doi: 10.1109/TIA.2017.2684086.

[5] M. Saur, D. Gaona, J. Zdravkovic, F. Hentschel, R. D. Lorenz, and D. Gerling, "Experimental evaluation of iron loss minimization in automotive traction drives by increased disturbance rejection and precise flux control," 2016 19th International Conference on Electrical Machines and Systems (ICEMS), Chiba, 2016, pp. 1-6.

[6] J. S. Lee and R. D. Lorenz, "Deadbeat Direct Torque and Flux Control of IPMSM Drives Using a Minimum Time Ramp Trajectory Method at Voltage and Current Limits," in IEEE Transactions on Industry Applications, vol. 50, no. 6, pp. 3795-3804, Nov.-Dec. 2014, doi: 10.1109/TIA.2014.2322131.

[7] J. S. Lee, R. D. Lorenz and M. A. Valenzuela, "Time-Optimal and Loss-Minimizing Deadbeat-Direct Torque and Flux Control for Interior Permanent-Magnet Synchronous Machines," in IEEE Transactions on Industry Applications, vol. 50, no. 3, pp. 1880-1890, May-June 2014, doi: 10.1109/TIA.2013.2287313.

[8] J. S. Lee and R. D. Lorenz, "Robustness Analysis of Deadbeat-Direct Torque and Flux Control for IPMSM Drives," in IEEE Transactions on Industrial Electronics, vol. 63, no. 5, pp. 2775-2784, May 2016, doi: 10.1109/TIE.2016.2521353.

[9] H. El Khatib, M. Peña, B. Grothmann, E. Gedlu, and M. Saur, "Applying the Square-Root-Condition combined with DB-DTFC as a Flux Observer-Based Maximum Torque per Flux Strategy," 2019 IEEE 10th International Symposium on Sensorless Control for Electrical Drives (SLED), Turin, Italy, 2019, pp. 1-6, doi: 10.1109/SLED.2019.8896256.

[10] N. T. West and R. D. Lorenz, "Digital Implementation of Stator and Rotor Flux-Linkage Observers and a Stator-Current Observer for Deadbeat Direct Torque Control of Induction Machines," in IEEE Transactions on Industry Applications, vol. 45, no. 2, pp. 729-736, March-April 2009, doi: 10.1109/TIA.2009.2013567.

[11] G. Pellegrino, E. Armando, and P. Guglielmi, "Direct-Flux Vector Control of IPM Motor Drives in the Maximum Torque Per Voltage Speed Range," in IEEE Transactions on Industrial Electronics, vol. 59, no. 10, pp. 3780-3788, Oct. 2012, doi: 10.1109/TIE.2011.2178212.

[12] B. Boazzo and G. Pellegrino, "Model-Based Direct Flux Vector Control of Permanent-Magnet Synchronous Motor Drives," in IEEE Transactions on Industry Applications, vol. 51, no. 4, pp. 3126-3136, July-Aug. 2015, doi: 10.1109/TIA.2015.2399619.

[13] M. S. Petit, B. Sarlioglu, R. D. Lorenz, B. S. Gagas and C. W. Secrest, "Deadbeat Flux Vector Control for Dynamic Six-Step Operation of Synchronous Machines," *2019 IEEE Transportation Electrification Conference and Expo (ITEC)*, Detroit, MI, USA, 2019, pp. 1-6. doi: 10.1109/ITEC.2019.8790528

[14] M. S. Petit, B. Sarlioglu, R. D. Lorenz, B. S. Gagas, and C. W. Secrest, "Spatial Deadbeat Torque Control for Six-Step Operation," *2019 IEEE Energy Conversion Congress and Exposition (ECCE)*, Baltimore, MD, USA, 2019, pp. 2380-2387.
doi: 10.1109/ECCE.2019.8912507

[15] D. Gaona, H. El Khatib, T. Long, and M. Saur, "Overmodulation Strategy for Deadbeat-Flux and Torque Control of IPMSM with Flux Trajectory Control in the Stationary Reference Frame," *2020 IEEE Energy Conversion Congress and Exposition (ECCE)*, Detroit, MI, USA, 2020.